Int. J. Electrochem. Sci., 8 **(2013)** 6145 - 6153

International Journal of
ELECTROCHEMICAL
SCIENCE
www.electrochemsci.org

Conductivity Enhancement of (Epoxidized Natural Rubber 50)/Poly(Ethyl Methacrylate)–Ionic Liquid-Ammonium Triflate

S.F. Mohammad[1], *N. Zainal*[1,2,*], *S. Ibrahim*[1] *and N.S. Mohamed*[2,*]

[1] Institude of Graduate Studies, University of Malaya
[2] Centre for Foundation Studies in Science, University of Malaya
*E-mail: nlin@um.edu.my, nsabirin@um.edu.my

Received: 26 November 2012 / *Accepted:* 28 December 2012 / *Published:* 1 May 2013

The present work investigates the role of ionic liquid, 1-butyl-3 methyl imidazolium tetrafluoroborate in enhancing the conductivity of polymer electrolyte system of epoxidized natural rubber 50/poly(ethyl methacrylate)-ammonium triflate. Fourier transform infrared spectroscopic study shows evidence of interaction between epoxidized natural rubber 50, poly(ethyl methacrylate), ionic liquid and ammonium salt. Addition of ammonium salt to the epoxidized natural rubber 50/poly(ethyl methacrylate)-ionic liquid system increases the glass transition temperature indicating reduction in flexibility of the host polymer chains due to formation of transient cross-linking. However, the room temperature ionic conductivity of the polymer electrolyte increases with salt content about an order of magnitude compared to the system without ionic liquid. The results of this work show that the ionic liquid in this polymer electrolyte system acts as plasticizer which assists dissolution and dissociation of the doping salt, resulting in higher concentration of charge carriers. The activation energy result reveals that the presence of ionic liquid weakens the interactions between polymer chains and cation from the ammonium salt.

Keywords: Epoxidized natural rubber; ionic liquid; ammonium triflate

1. INTRODUCTION

Solid polymer electrolytes (SPEs) have attracted considerable attention due to their successful use in electrochemical devices such as batteries, supercapacitors and electrochromic devices [1-3]. Some of the advantages of solid polymer electrolyte systems compared to liquid electrolyte are the possibility of fabrications in various shapes, low self-discharge, compact and leakage free [4].

Substantial effort has been devoted to improve the performance of SPEs including the use of variety of host polymers. Polymer electrolytes based on natural rubber (NR) are among promising materials used in the field of polymer electrolyte. Diversification of the conventional uses of NR has been achieved by changing the properties of the polymer through chemical modifications. One of the popular types of modified natural rubber is epoxidized natural rubber (ENR) which is produced by epoxidation of NR. The presence of oxygen in the epoxy groups of the ENR facilitates the motion of cation when it is doped with dopant salts [5].

Among three types of ENR produced in Malaysia, ENR-50 is the most studied for use as host in polymer electrolyte. ENR-50 is a polymer with soft elastomeric, good elasticity and adhesive properties. However, pure ENR-50 films are very soft, tacky and difficult to handle. To overcome this problem, ENR-50 is commonly blended with other polymer such as, PVC, PMMA, PEO and PVDF [6-9]. Poly (ethyl methacrylate) (PEMA) is one the polymer that attracted the attention of many groups of researchers [10-12]. PEMA is one the polymers which have methacrylic ester in their chemical structures [12]. This methacrylic ester polymer has an excellent chemical resistance, high surface resistivity and mechanical properties.

Due to good compatibility of PEMA with many polymers, the authors have prepared ENR-50/PEMA blend added with ammonium triflate ($NH_4CF_3SO_3$) and obtained flexible free-standing films. The highest conductivity achieved is in the order of 10^{-6} S cm^{-1} [13]. However, this conductivity is low and not suitable for practical application. With the objective to enhance the conductivity of the ENR-50/PEMA-$NH_4CF_3SO_3$, the present work was undertaken by adding ionic liquid, 1-butyl-3 methyl imidazolium tetrafluoroborate ($BMI{\cdot}BF_4$) to the system. Investigation on the effect of the ionic liquid to the conductivity enhancement, the ENR-50/PEMA-$NH_4CF_3SO_3$ added with $BMI{\cdot}BF_4$ was characterized using impedance spectroscopy. In order to account for the change in conductivity caused by the ionic liquid, fourier transform infrared (FTIR) spectroscopy and differential scanning calorimetry (DSC) were also performed.

2. EXPERIMENTAL

Polymer electrolyte samples were prepared by solution casting technique. The ENR-50 supplied by Rubber Research Institute, Malaysia was used as the polymer host. PEMA (Aldrich), tetrahydrofuran (THF), $NH_4CF_3SO_3$ (Aldrich) and $BMI{\cdot}BF_4$ (Aldrich) were used without purification.

In this work, polymer films of ENR-50/PEMA-$BMI{\cdot}BF_4$ containing different wt.% of $NH_4CF_3SO_3$ were prepared. For preparing the polymer films, ENR-50 and PEMA were first dissolved in THF at 40°C for 72 hours to form homogeneous solutions. The ratio of ENR-50 to PEMA was fixed at 60:40 of wt.%. The reason for choosing this ratio is explained in Mohammad et al [13]. Ionic liquid of suitable amount was then added into ENR-50/PEMA solution. Finally, a desired amount of $NH_4CF_3SO_3$ was added. Then, the solution was cast into petri dishes and left to dry to form electrolyte films. To eliminate excess THF, the films were further dried in a vacuum oven at 40°C for 2 days.

Fourier transform infrared (FTIR) spectroscopy was used to study interactions between constituents of polymer electrolytes. Such interactions could be manifested through FTIR spectra as frequency shifts, band intensity changes, splitting of bands and alteration of band shapes. In this work, FTIR was carried out using PerkinElmer Spectrum 400 FT Mid-IR/Far-IR spectrometer. The FTIR spectra were recorded in the range from 4000 to 400 cm^{-1} in the transmittance mode with a resolution of 2 cm^{-1}. Thermal study from differential scanning calorimetry (DSC) data was obtained using the Mettler Toledo $DSC822^e$ equipped with an intra-cooler. Samples of about 4-5 mg were placed in hermitically sealed 40 µl aluminium crucibles in a self-generated atmosphere. The self-generated atmosphere was obtained by piercing 50 µm holes in the aluminium lid of a sealed crucible. The samples were heated from -65°C to 170°C at 10°C min^{-1} and then cooled from 170°C to -65°C at 10°C min^{-1} under nitrogen condition.

To find the ionic conductivity of the polymer electrolyte materials, impedance measurements were done using a HIOKI 3532-50 Hi Tester analyzer. The sample was first cut into a suitable size. The sample was then mounted between two electrodes of diameter 2 cm. The impedance measurements were carried out at different temperatures from room temperature up to 80ºC. The conductivity of the samples was calculated using the equation:

$$\sigma = \frac{t}{R_b A_o} \qquad (1)$$

where R_b is the bulk resistance obtained from the intercept on the real impedance axis, t is the thickness of sample and A_o is the area of blocking electrode.

3. RESULTS AND DISCUSSION

3.1 Interaction between constituents

FTIR was performed to confirm the interactions between the constituents in the polymer electrolyte materials.

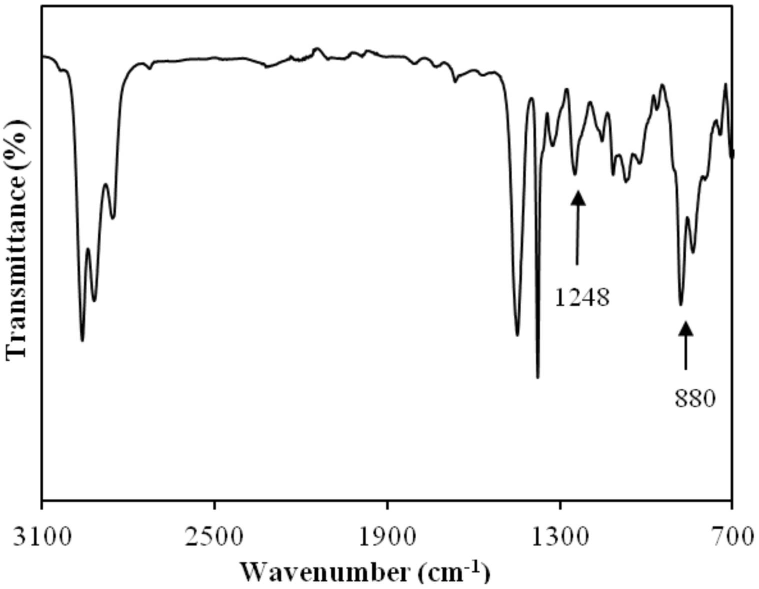

Figure 1. FTIR spectrum of ENR-50 in the spectral region between 3100 and 700 cm^{-1}

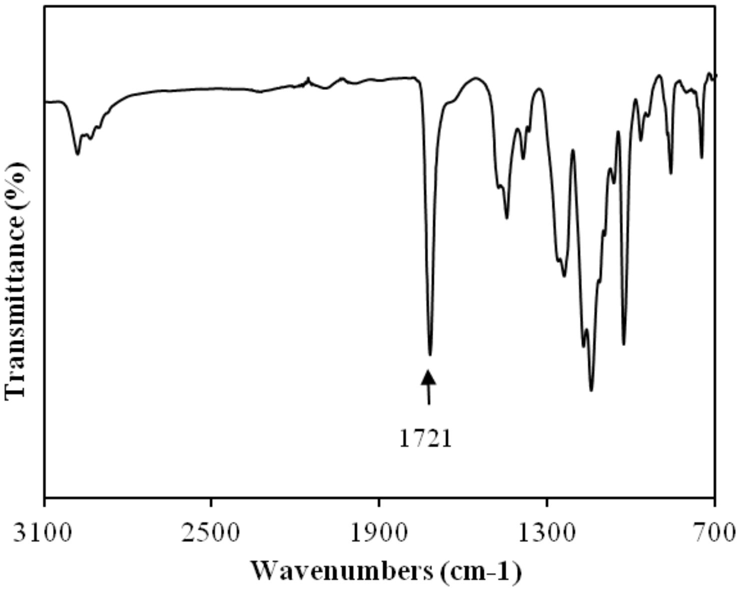

Figure 2. FTIR spectrum of PEMA in the spectral region between 3100 and 700 cm^{-1}

Fig. 1 presents the FTIR spectrum of pure ENR-50 in the region from 3100 to 700 cm^{-1} while Fig. 2 shows the FTIR spectrum of PEMA film in the spectrum region from 3100 to 700 cm^{-1}. The spectrum in Fig. 1 exhibits the epoxide groups (C-O-C) of ENR-50 at 1248 and 880 cm^{-1} [14], while the spectrum in Fig. 2 reveals the carbonyl group (C=O) of PEMA at 1721 cm^{-1} [15]. The spectrum of BMI·BF$_4$ ionic liquid (in the spectral region from 3500-500 cm^{-1}) is displayed in Fig. 3. The observed spectral bands can be assigned to the C-N, C-H stretching vibration modes of the imidazolium ring (3162, 3122, 2965, 2939 and 2878 cm^{-1}), asymmetric stretching vibrations of BF$_4^-$ (1033 cm^{-1}) and C-H bending vibrations of imidazolium ring (755 and 623 cm^{-1}) [16].

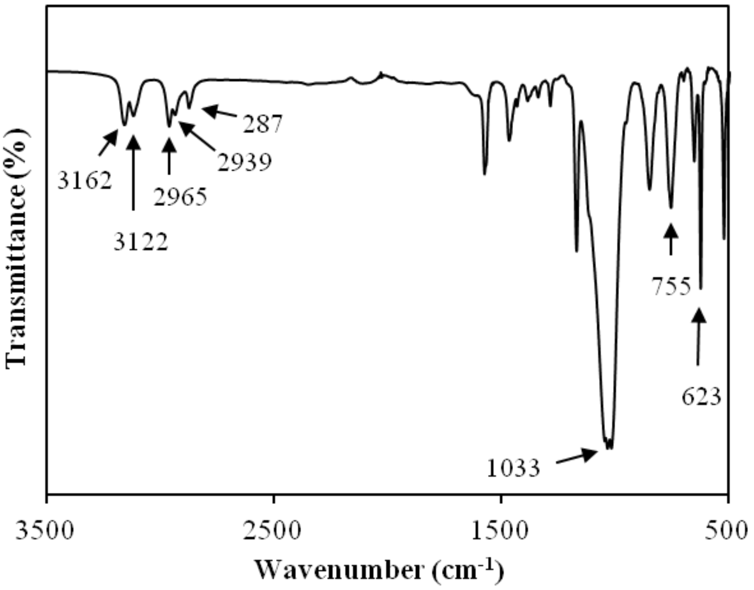

Figure 3. FTIR spectrum of BMI·BF$_4$ in the spectral region from 3500 to 500 cm^{-1}

The FTIR spectra of $BMI\cdot BF_4$, ENR-50/PEMA blend, ENR-50/PEMA-$NH_4CF_3SO_3$ and ENR-50/PEMA-$BMI\cdot BF_4$-$NH_4CF_3SO_3$ in different spectral regions are displayed in Fig. 4. The presence of anion-cation of $BMI\cdot BF_4$ in the polymer electrolyte system can be studied by observing the vibrational modes of the anion-cation. Fig. 4a depicts the spectra of $BMI\cdot BF_4$, (ENR-50)/PEMA, (ENR-50)/PEMA-$NH_4CF_3SO_3$ and (ENR-50)/PEMA-$BMI\cdot BF_4$-$NH_4CF_3SO_3$ in the region between 3400-2500 cm^{-1}. This is the region where the C-N and C-H stretching vibration modes of the imidazolium ring from the $BMI\cdot BF_4$ is situated. The bands of C-H (Fig. 4a(i)) at 3162 and 2965 cm^{-1} shifted to higher wavenumbers of 3170 and 2972 cm^{-1} in the spectrum of Fig. 4a(iv).

From Fig. 4b, the doublet peaks at 1033 and 1016 cm^{-1} which correspond to BF_4 asymmetric stretching vibrations disappeared while the peak at 1029 cm^{-1} (Fig. 4b(iii)) becomes more intense with addition of the ionic liquid. The band at 623 and 755 cm^{-1} which are attributed to out of plane C-H bending vibrations of imidazolium ring are not observable in the spectrum of electrolyte containing the ionic liquid, Fig. 4c(iv). The bands at 760 and 747 cm^{-1} are shifted to 759 and 746 cm^{-1} while the band at 640 cm^{-1} is shifted to 638 cm^{-1} with the addition of ionic liquid. The changes mentioned above give indications of interactions between ENR-50/PEMA-$NH_4CF_3SO_3$ electrolyte systems with anion-cation from $BMI\cdot BF_4$.

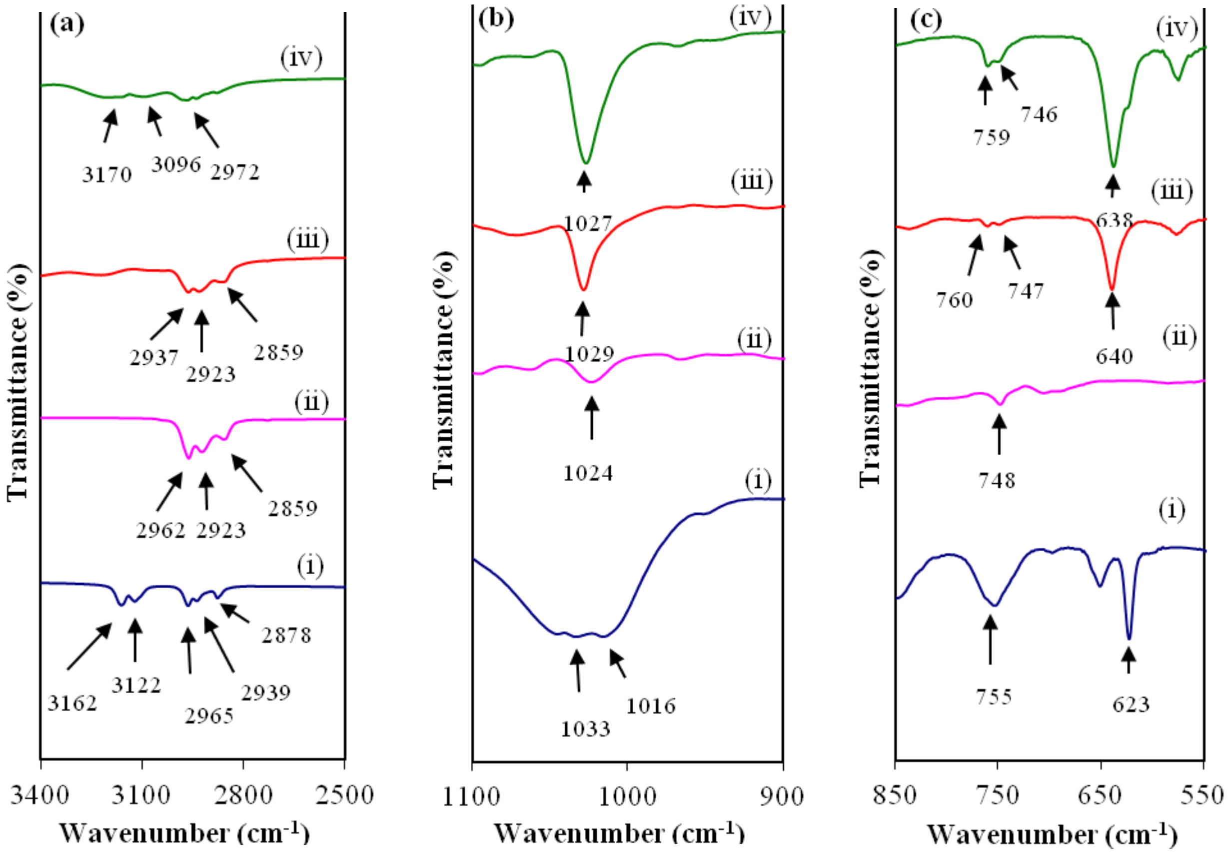

Figure 4. FTIR spectra in the spectral region (a) 3400-2500 cm^{-1}, (b) 1100-900 $cm^{-1}$and (c) 850-550 cm^{-1} for (i) $BMI\cdot BF_4$, (ii) ENR-50/PEMA (iii) ENR-50/PEMA-$NH_4CF_3SO_3$ and (iv) (ENR-50)/PEMA-$BMI\cdot BF_4$-$NH_4CF_3SO_3$.

3.2 Thermal analysis

Thermal study was carried out using DSC measurement to determine the glass transition temperature, T_g of the polymer electrolyte materials. Fig. 5 illustrates DSC profiles of ENR-50/PEMA-BMI·BF_4-$NH_4CF_3SO_3$ electrolyte system. According to Zhang et al [17] the T_g for BMI·BF_4 is 202.15 K. The DSC profiles show single glass transition temperature, which shows the miscibility of the ionic liquid with ENR-50/PEMA-$NH_4CF_3SO_3$ electrolyte [18]. The DSC profiles also show increasing trend of T_g with increasing amount of $NH_4CF_3SO_3$. The trend of T_g with salt content is attributable to transient cross-linking between the H^+ ions of $NH_4CF_3SO_3$, anion-cation of ionic liquid and epoxy group of ENR-50 in the polymer matrix [19-23]. The presence of interactions between ENR-50/PEMA-$NH_4CF_3SO_3$ and BMI·BF_4 ionic liquid is proven by the changes of vibrational bands in the ENR-50/PEMA-BMI·BF_4-$NH_4CF_3SO_3$ as discussed earlier.

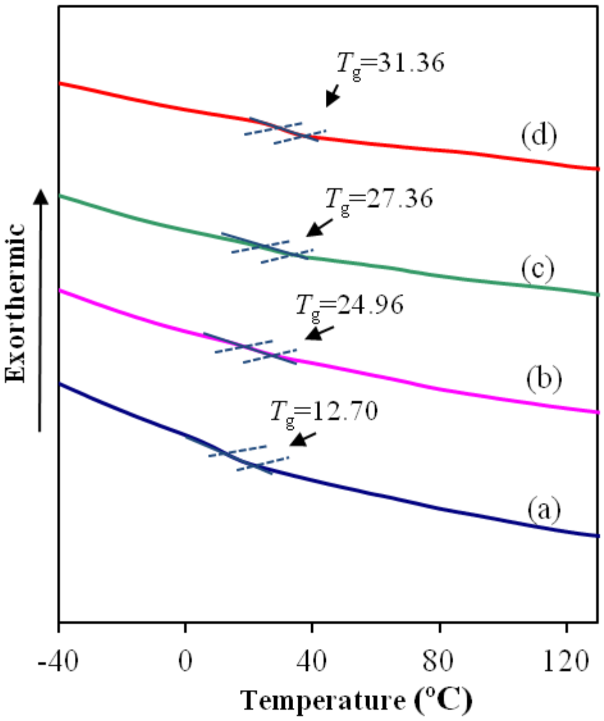

Figure 5. DSC curves for ENR-50/PEMA-BMI·BF_4 electrolytes at (a) 20 wt.%, (b) 30 wt.%, (c) 35 wt.% and (d) 40 wt.% of $NH_4CF_3SO_3$

3.3 Conductivity studies

The variation of room temperature conductivity of ENR-50/PEMA-BMI·BF_4-$NH_4CF_3SO_3$ electrolyte system as a function of $NH_4CF_3SO_3$ content is presented in Fig. 6. The conductivity increases with increase in $NH_4CF_3SO_3$ content. Comparing with the BMI·BF_4 free ENR-50/PEMA containing the same content of $NH_4CF_3SO_3$ [13], the BMI·BF_4 added ENR-50/PEMA shows higher conductivity value. In the ENR-50/PEMA-BMI·BF_4-$NH_4CF_3SO_3$ electrolyte systems, both cations and anions were expected to be mobile and thus contribute to the overall value of conductivity [24].

However, according to Vuk et al [25], conduction in imidazolium based compounds occurred via Grotthuss mechanism which depends on the movement of protons between neighbouring imidazolium cations. As such, the presence of the ionic liquid in the ENR-50/PEMA-$NH_4CF_3SO_3$ complex might have provided new conductivity pathways for ions, leading to an increase in conductivity. The increase in ionic conductivity of the ENR-50/PEMA-BMI·BF_4-$NH_4CF_3SO_3$ system could also be ascribed to the excess production of different types of ions, as ionic liquid consists of BMI cations and BF_4 anions [26]. High concentration of these charge carriers enhanced the dissociation of $NH_4CF_3SO_3$. This implies that BMI·BF_4 also acted as a plasticizer that modified the system by assisting the dissolution and dissociation of the doping salt and thus produced more charge carriers [27].

The highest ionic conductivity in the order of 10^{-5} S cm^{-1} is obtained for the film containing 40 wt. % of $NH_4CF_3SO_3$. Since the increase in salt content increases T_g value, the enhancement in the ionic conductivity with increasing salt is not associated with increase in segmental motion of the polymer host but is possibly due to an increase in number of carrier ions [18].

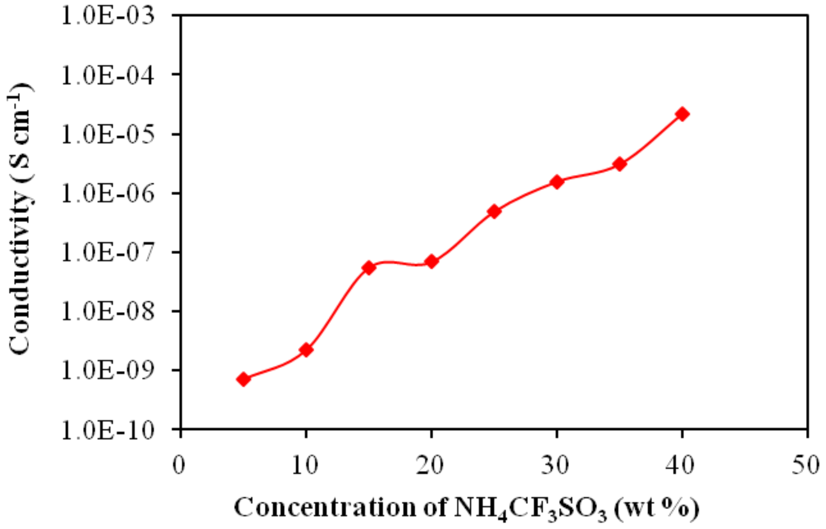

Figure 6. Conductivity against wt.% of $NH_4CF_3SO_3$ at room temperature.

Temperature dependent ionic conductivity measurement was carried out to analyse the mechanism of ionic conduction in polymer electrolyte. The ionic conductivity as a function of temperature is depicted in Fig. 7. From Fig. 7, the temperature dependence-conductivity data is best fitted by the empirical Vogel-Tamman-Fulcher (VTF). The graph for the sample with 40 wt% of $NH_4CF_3SO_3$ shows a modest increase in ionic conductivity from ambient temperature to 80 °C, reaching the ionic conductivity of 8.08×10^{-4} S cm^{-1} at 80 °C. The trend of temperature dependent conductivity, suggests that ion transport in ENR-50/PEMA-$NH_4CF_3SO_3$ electrolyte system is nominated by mobility of host chains.

The activation energy, E_a, for the ENR-50/PEMA-BMI·BF_4-$NH_4CF_3SO_3$ electrolytes was determined from the gradient of the VTF plots in Fig. 7. The E_a values of the electrolyte system are listed in Table 1. It is known that ionic conductivity is proportional to the concentration of charge carriers and migration rate of charge carriers that is related to E_a [27]. The decrease in E_a as listed in

Table 1 shows an increase in ionic mobility which in turn increases ionic conductivity. The values of E_a in ENR-50/PEMA-BMI·BF_4-$NH_4CF_3SO_3$ electrolyte system are lower than the values of E_a obtained in electrolyte system without containing ionic liquid [13]. This could possibly due to the presence of BMI·BF_4 that disrupted and weakened the interaction between the polymer chain and H^+ in ammonium ions. As such, low energy is required to break the bond of the ion from the donor sites.

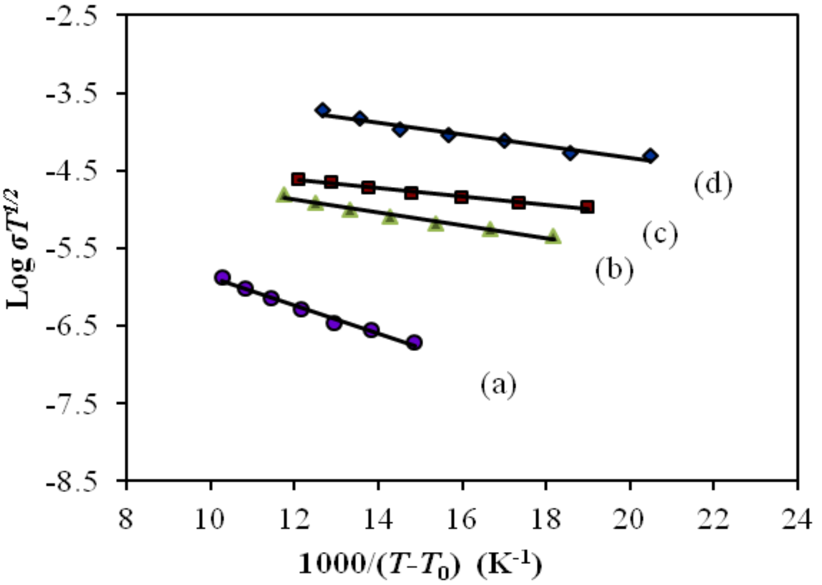

Figure 7. VTF plots of ENR-50/PEMA-BMI·BF_4 added with (a) 20 wt.%, (b) 30 wt.%, (c) 35 wt.% and (d) 40 wt.% of $NH_4CF_3SO_3$.

Table 1. Ionic conductivity and activation energy values for ENR 50/PEMA-BMI·BF_4-$NH_4CF_3SO_3$ electrolyte system

Sample (in wt.% of $NH_4CF_3SO_3$)	Ionic conductivity, σ (S cm^{-1}) at room temperature	Activation energy, E_a (×10^{-2} eV)
20	6.93×10^{-8}	1.827
30	1.55×10^{-6}	0.817
35	3.12×10^{-6}	0.739
40	2.20×10^{-5}	0.713

4. CONCLUSION

Addition of BMI·BF_4 enhanced conductivity of ENR-50/PEMA-$NH_4CF_3SO_3$ about an order of magnitude. The enhancement of conductivity is attributed to the presence of ionic liquid that acts as plasticizer which assists the dissolution and dissociation of the doping salt and thus produced more charge carriers. The presence of the ionic liquid in the ENR-50/PEMA-$NH_4CF_3SO_3$ also disrupts and weakens interactions between chains of polymer with H^+ from the ammonium triflate which in turns reducing the energy required to break the bond of the H^+ from the donor sites. This is indicated by the lower E_a value of the system compared to that without the ionic liquid.

References

1. C.P. Fonseca and S. Neves, *J. Power Sources*, 159 (2006) 712.
2. G.P. Pandey, Y. Kumar and S.A. Hashmi, *Indian J. Chem.*, 49A (2010) 743.
3. J. Reiter, O. Krejza and M. Sedlarikova, *Solar Energy Materials & Solar Cells,* 93 (2009) 249.
4. T. Kuila, S.K. Srivastava, H. Acharya, B.K. Samantary and C. Kureti, *Materials Science and Engineering B*, 137 (2007) 217.
5. H.S. Kim, R. Idris and S.I. Moon, *Bull. Electrochem.,* 20 (2004) 465.
6. A. Ahmad, M.Y.A. Rahman, M.L.M. Ali, H. Hashim and F.A. Kalam, *Ionics,* 13 (2007) 67.
7. F. Latif, M. Aziz, N. Katun, A.M.M. Ali, and M.Z.A. Yahya, *J. Power Sources,* 159 (2006) 1401.
8. S.A.M. Noor, A. Ahmad, I.A. Talib and M.Y.A. Rahman, *Ionics,* 16 (2010) 161.
9. M. Aziz and C.L. Chew, *Solid State Science and Technology,* 13 (2005) 126.
10. T. Fahmy and M.T. Ahmed, *Polymer Testing,* 20 (2001) 477.
11. E.M. Abdelrazek, *Physica B,* 400 (2007) 26.
12. M. Sivakumar, R. Subadevi, S. Rajendran, H.C. Wu and N.L. Wu, *European Polymer Journal*, 43 (2007) 4466.
13. S.F. Mohammad, R. Idris and N.S. Mohamed, *Advanced Materials Research: Material and Manufacturing Technology* 129-131 (2010) 61.
14. S.N. Gan and Z.A. Hamid, Polymer, 38 (1997) 1953.
15. S. Rajendran, M.P. Ramesh and M.R. Usha, Journal of Power Sources, 180 (2008) 880.
16. G. Lakshminarayana and M. Nogami, Solid State Ionics, 181 (2010) 760.
17. S. Zhang, N. Sun, X. He, X. Lu and X. Zhang, *J. Phys. Chem. Ref. Data,* 35 (2006) 1475.
18. E. Marwanta, T. Mizumo, N. Nakamura and H. Ohno, *Polymer,* 46 (2005) 3795.
19. B.E. Mellander and I. Albinsson, *Ionics,* 4 (1998) 415.
20. W. Klinklai, S. Kawahara, E. Marwanta, T. Mizumo, Y. Isono and H. Ohno, *Solid State Ionics,* 177 (2006) 3251.
21. N.K. Karan, D.K. Pradhan, R. Thomas, B. Natesan and R.S. Katiyar, *Solid State Ionics*, 179 (2008) 689.
22. N. Zainal, R. Idris and N.S. Mohamed, *Adv. Mater. Res.,* 287-290 (2011) 424.
23. N. Zainal, R. Idris and N.S. Mohamed, *Adv. Mater. Res.*, 545 (2012) 303.
24. S.S. Sekhon, P. Krishna, B. Singh, K. Yamada and C.S. Kim, *Electrochim. Acta,* 52 (2006) 1639.
25. S.A. Vuk, V. Jovanovski, A. Pollet-Villard, I. Jerman and B. Orel, *Solar Energy Materials and Solar Cells*, 92 (2008) 126.
26. P.K. Singh, K.W. Kim and H.W. Rhee, *Electroshem. Commun.*, 10 (2008) 1769.
27. S. Ramesh, C.W. Liew and K. Ramesh, *J. Non-Crystalline Solids,* 357 (2011) 2132.